



Titre: Combining Pulsed and DC Gradients in a Clinical MRI-Based
Title: Microrobotic Platform to Guide Therapeutic Magnetic Agents in the
Vascular Network

Auteurs: Sylvain Martel
Authors:

Date: 2013

Type: Article de revue / Article

Référence: Martel, S. (2013). Combining Pulsed and DC Gradients in a Clinical MRI-Based
Citation: Microrobotic Platform to Guide Therapeutic Magnetic Agents in the Vascular
Network. International Journal of Advanced Robotic Systems, 10(1).
<https://doi.org/10.5772/53513>

 **Document en libre accès dans PolyPublie**
Open Access document in PolyPublie

URL de PolyPublie: <https://publications.polymtl.ca/3432/>
PolyPublie URL:

Version: Version officielle de l'éditeur / Published version
Révisé par les pairs / Refereed

Conditions d'utilisation: Creative Commons Attribution 4.0 International (CC BY)
Terms of Use:

 **Document publié chez l'éditeur officiel**
Document issued by the official publisher

Titre de la revue: International Journal of Advanced Robotic Systems (vol. 10, no. 1)
Journal Title:

Maison d'édition: Sage Publications
Publisher:

URL officiel: <https://doi.org/10.5772/53513>
Official URL:

Mention légale:
Legal notice:

Combining Pulsed and DC Gradients in a Clinical MRI-Based Microrobotic Platform to Guide Therapeutic Magnetic Agents in the Vascular Network

Regular Paper

Sylvain Martel^{1,*}

¹ NanoRobotics Laboratory, Department of Computer and Software Engineering, École Polytechnique de Montréal (EPM), Montréal, Canada
* Corresponding author E-mail: sylvain.martel@polymtl.ca

Received 9 Jun 2012; Accepted 18 Sep 2012

DOI: 10.5772/53513

© 2013 Martel; licensee InTech. This is an open access article distributed under the terms of the Creative Commons Attribution License (<http://creativecommons.org/licenses/by/3.0>), which permits unrestricted use, distribution, and reproduction in any medium, provided the original work is properly cited.

Abstract Magnetic Resonance Navigation (MRN) relies on the use of an upgraded clinical Magnetic Resonance Imaging (MRI) scanner to navigate therapeutic, imaging, or diagnostic magnetic micro-agents in the vascular network. Although the high homogeneous field in the tunnel of the MRI scanner increases the magnetization of the navigable agents towards full saturation, the magnetic gradients superposed on such a high homogeneous field, generated by the Imaging Gradient Coils (IGC) typically used for MR-image slice selection, allow the induction of pulling forces to steer such agents in the targeted branches at the vessel's bifurcations. However, increasing the magnitude of such gradients leads to a significant decrease of the duty cycle, leading to a substantial reduction of the effective steering force being applied. To increase such a duty cycle, a Steering Gradient Coils (SGC) assembly capable of higher magnitudes while maintaining a 100% duty cycle can be installed at the cost of a much slower slew rate. Here, the use and the potential effectiveness of IGC and/or SGC for guiding such agents are briefly investigated on the basis of known specifications and experimental data.

Keywords Magnetic Resonance Imaging, Navigable Agents, Magnetic Force, Targeted Therapies and Diagnostics, Vascular Network

1. Introduction

For some types of cancer, enhanced therapeutic efficacy can be obtained by direct targeting, where a minimal dose of drug-loaded microcarriers or agents can be navigated through the shortest route in the vascular network while avoiding or at least reducing systemic circulation, which most often leads to a substantial increase in secondary toxicity that may affect healthy organs [1]. Direct targeting requires the assistance of a more sophisticated interventional platform and engineering techniques that also rely on the synthesis of navigable therapeutic agents and the associated medical interventional protocols.

One such promising interventional platform relies on a clinical Magnetic Resonance Imaging (MRI) scanner that

is upgraded to allow Magnetic Resonance Navigation (MRN) [2] of these navigable agents along a planned trajectory in the vasculature in order to achieve direct targeting. MRN has already been tested successfully *in vivo* in the carotid artery of a living pig with a 1.5 mm chrome-steel bead and a clinical MRI scanner using the Imaging Gradient Coils (IGC) to propel the bead back and forth along the artery in a controlled fashion [3]. Later, ~50 μm therapeutic agents known as Therapeutic Magnetic MicroCarriers (TMMC) were navigated through the hepatic artery of rabbit models to reach targeted locations in the liver [4]. In these experiments, TMMC consisted of therapeutics (Doxorubicin) embedded with FeCo magnetic nanoparticles (MNP) within a spherical biodegradable polymer (PLGA) matrix. The latter experiments were performed with a clinical MRI scanner upgraded with a special gradient coils assembly – referred to as Steering Gradient Coils (SGC) – installed inside the tunnel of the scanner. Unlike IGC, SGC were able to provide sustained (100% duty cycle) higher gradient fields, but with much slower slew rates. The experience acquired by performing MRN using IGC or SGC, referred to as IGC-MRN and SGC-MRN respectively, forced us to re-evaluate the limitations in relation to the advantages of each approach in the context of navigating therapeutic agents in the vascular network. This is the main objective of this paper. First, to better understand the principle of MRN, some theoretical background is necessary.

2. Fundamental Theory of MRN

The fundamental platform of MRN is the MRI scanner, which provides a high-magnitude homogenous magnetic field of typically 1.5 T or 3 T for clinical scanners known as the B_0 field, a magnetic gradient field that can be oriented in any direction and an RF field. For imaging, the momentum or spin of the hydrogen nuclei is aligned in the direction of the B_0 field, which corresponds to the z-axis and therefore $B_0 \equiv B_z$. An RF field is then applied momentarily to flip the spin angle. When the RF pulse is turned off, the spin returns to its original direction towards the z-axis during a time period known as the relaxation time. During this relaxation time, when the magnetic dipoles tend to align with the magnetic field, the scanner detects the re-emitted signals that are used to construct the MR-image. To select a particular region to be imaged, linear field gradients created by three sets of orthogonally positioned coils are superimposed on the B_0 field.

For MRN, a displacement of a magnetic agent can occur if a sufficiently high pulling force is induced, which can only occur with a magnetic field strength H provided by the B_0 field and a directional gradient G , where both are sufficiently high. In the z-axis, the magnetic field strength is related to the magnetic field

or magnetic flux density by the permeability of free space $\mu_0 = 4\pi \times 10^{-7} \text{ H/m}$:

$$B_z = \mu_0 H_z. \quad (1)$$

By inserting a ferromagnetic core with susceptibility χ in such a field, B_z is increased:

$$B_z = \mu_0(H_z + \chi H_z) = \mu_0(H_z + M_z). \quad (2)$$

In (2), M_z is the magnetization of the ferromagnetic material. For $B_z \geq 1.5 \text{ T}$, as in typical clinical MRI scanners, all ferromagnetic materials have their magnetization at saturation (especially in 3 T scanners) or very close to saturation (for 1.5 T scanners). Therefore, we assume here saturation magnetization where M_z is replaced by M_{sz} . In this case, the magnetic force induced by the MRI scanner on the navigable magnetic agent can be computed as

$$\vec{F}_M = D \cdot V_M (M_{sz} \cdot \nabla) B_z, \quad (3)$$

with the gradient operator being defined as

$$\nabla = \left[\frac{\partial}{\partial x} \quad \frac{\partial}{\partial y} \quad \frac{\partial}{\partial z} \right]^T. \quad (4)$$

In (3), the duty cycle D is the ratio of the duration τ of the applied magnetic gradient used to induce a directional pulling force F_M , referred to as the pulling gradient or steering gradient when the blood flow velocity is used to propel the navigable agent, to the total period T where D is included in the interval $[0, 1]$ with $D = 1$ representing a 100% duty cycle. Although the goal for providing the maximum pulling or steering force is to have $D \rightarrow 1$, several factors can reduce D , and one of the main factors beside the time taken for MR-tracking or imaging is the cooling issue. For IGC, the reduction in the duty cycle would depend on the magnitude of the gradient being generated, which would depend on the electrical current being applied on each axis (or channel) to generate a directional magnetic force:

$$\begin{bmatrix} F_{MX} \\ F_{MY} \\ F_{MZ} \end{bmatrix} = D \cdot V_M \cdot M_{sz} \begin{bmatrix} \frac{\partial B_x}{\partial z} & \frac{\partial B_y}{\partial z} & \frac{\partial B_z}{\partial z} \end{bmatrix}^T. \quad (5)$$

The next section provides different values of D for an IGC assembly capable of generating magnetic gradients in excess of $400 \text{ mT} \cdot \text{m}^{-1}$. Based on theoretical analysis and experiments this assembly is sufficient for the steering of MR-navigable therapeutic agents with diameters as small as ~50 μm in the arterioles under real human physiological conditions.

2. IGC-MRN

The main advantage of using the IGC for MRN is that the same coils can be used for both MR-tracking for gathering

positional data about the navigable agents for the servoing control purpose, and MR-steering of the agents towards the targeted region. For the IGC design used for MR-imaging (or tracking), several specifications are considered, such as linearity, self-inductance, resistance, stored energy, dissipated power, and external fields. Indeed, although non-linearity of the gradient results in image distortion, it is not as critical when used to generate steering gradients. The self-inductance is responsible for longer switching times (slower slew rates) and such self-inductance must be minimized for both cases, i.e., for MR-imaging or tracking and steering. This is also true for the stored energy in the gradient coil, which is defined as the squared amplitude of the magnetic field integrated over the volume of the coil, where such stored energy increases rapidly if the magnetic fields and the volume of the coil are increased, leading to a corresponding linear increase of the self-inductance. For a given electrical current circulating in the gradient coil, the dissipated power in the coil is proportional to the ohmic resistance, which should be minimized in both cases. Another aspect is eddy current induced in neighbored coils, which must be eliminated or at least minimized due to undesirable effects. Higher eddy currents are expected with stronger applied magnetic fields, greater electrical conductivity of the coils and/or faster switching gradients. As such, typical IGC assemblies include a shielding coil, concentric with the first coil but on a larger radius with an electrical current circulating in the opposite direction. This is referred to as active shielding. Active shielding leads to the need for more energy to maintain the same gradient field while requiring more volume to implement the IGC assembly. But increasing the magnitude of the gradient field can be beneficial for imaging (or tracking) and steering. For MR-imaging, such an increase would lead to thinner slices or image planes and an increase in spatial resolution while providing higher pulling forces for steering purpose.

But power dissipation is a real constraint when operating IGC at high magnitudes. For instance, let us consider an actively shielded IGC with an inner and external diameter of 150 mm and 240 mm, respectively, which can be placed inside the tunnel of a Siemens Magnetom Sonata clinical MRI scanner. The IGC is powered by its own set of amplifiers such that no software or hardware modifications on the clinical scanner are required for operations with magnetic gradients at least ten times those generated by the IGC of the clinical scanner while taking advantage of its B_0 field of 1.5T. This removable IGC is capable of generating a maximum gradient of $450 \text{ mT} \cdot \text{m}^{-1}$ with a rise time of $100 \mu\text{s}$. But by doing so, D will be decreased substantially in order to maintain the internal temperature within the operational limit characterized at 45°C above an ambient temperature of 20°C , assuming that water cooling of the IGC happens at 5.0

litres per minute at 32.5 psi in order to maintain the maximum heat dissipation of the IGC assembly at 500 W. The effect of the gradient strength on the duty cycle for $T = 1\text{s}$, which corresponds to one cardiac cycle or one cycle of pulsatile blood flow, is depicted in Fig. 1, in which only one of the three channels (x, y, z) is active at any instant.

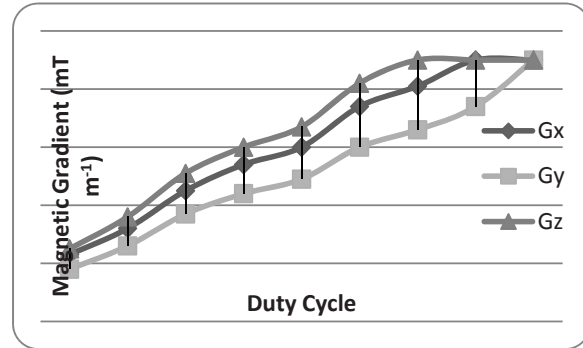


Figure 1. Reduction of the duty cycle with higher gradient fields for each axis generated by the removable IGC with only one axis being active at any instant

For instance, to guarantee a gradient of $450 \text{ mT} \cdot \text{m}^{-1}$ in any directions, $D = 0.043$, which corresponds to a duration τ of the applied magnetic gradient of only 43 ms every second. A burst mode where several gradient pulses are applied within the same T is possible as long as the power dissipation is kept within the operational limit. In such a case, the magnitude of the gradients could be decreased in order to maintain the internal temperature of the IGC within acceptable limits.

However, the slew rate dB/dt at such higher gradients can pose a threat to the patient [5] knowing that the mean threshold levels are 60 T/s for peripheral nerve sensation, 90 T/s for peripheral nerve pain, 900 T/s for respiratory system stimulation, and 3600 T/s for cardiac stimulation [6]. Presently, for clinical practices the FDA guidelines suggest 0-20 T/s, which limits gradient switching rates to a factor of 3 below the mean Peripheral Nerve Stimulation (PNS) level ($> 20 \text{ T/s}$ for first and second controlled modes, limited by human ethics committees). The typical operating range for MR-imaging is 45 T/s, which suggests maximum gradient amplitudes of $90 \text{ mT} \cdot \text{m}^{-1}$ for a maximum adequate rise time of $200 \mu\text{s}$ for MRI sequencing. For IGC-MRN sequencing using $450 \text{ mT} \cdot \text{m}^{-1}$, the minimum acceptable rise time becomes 11.25 ms, which translates to a maximum possible switching frequency (assuming that no MR-tracking is performed) of 44.44 Hz. For operating within the FDA recommendations of 0-20 T/s, these figures become 22.5 ms and 22.22 Hz. At the limit of this IGC, i.e., for an increase from 0 to $450 \text{ mT} \cdot \text{m}^{-1}$ in $100 \mu\text{s}$, the switching rate would correspond to 450 T/s, which is well above the threshold for peripheral nerve pain but still well below the threshold for respiratory system stimulation.

However, it is known that the induced current produced by such gradients in the patient is proportional not only to the slew rate but also to the cross-sectional area of the body being exposed to such a varying magnetic field; therefore, the orientation of the steering gradients could be considered in evaluating the risks for the patient. But smaller IGC, such as head-only gradient coils, can gain safety/sensory threshold margins due both to their reduced length and the reduced cross-sectional area over which the gradients occur. The gradient efficiency scales with the fifth power of the radius, so that reducing the diameter of the IGC two-fold can increase the gradient strength by a factor of 32. Therefore, a smaller IGC not only enables the use of larger amplitudes with good safety margins, but also makes such high gradients practical to implement.

3. SGC-MRN

The main advantage of installing an SGC inside the tunnel of a clinical MRI scanner that requires no software or hardware modification of the scanner, is the fact that the duty cycle can be maintained at 100% of maximum gradient fields, i.e., $D = 1$. But because the SGC assembly is driven by three DC power supplies (one for each axis), the slew rate is much lower than for the pulsed gradients generated through the IGC. For instance, for a gradient of $450 \text{ mT} \cdot \text{m}^{-1}$, the rise time was $100 \mu\text{s}$ (extended to 22.5 ms to be within FDA guidelines) and $\sim 350 \text{ ms}$ (measured experimentally) during IGC-MRN and SGC-MRN, respectively. Such a long rise time prevents the SGC from being used as imaging coils and, more importantly, puts a constraint on MR-imaging or MR-tracking during MRN. This is due to interferences between the SGC and the IGC, whereby the SGC must be set back to zero prior to MR-tracking for gathering positional information for servoing control.

Because of the slow switching mode, SGC-MRN would be more appropriate over IGC-MRN when the steering gradient must be maintained for a longer time period than would be possible with the IGC and where a relatively fast directional change of the gradient is not required. This would imply open-loop MRN where servoing would not be necessary, or servoing MRN that does not operate under tight real-time constraints. Another intervention that can take full advantage of the SGC is magnetically guided catheterization. Indeed, a gradient acting on a magnetically steered catheter or guidewire must typically be maintained longer than the duty cycle of the IGC at high gradients until the tip of the catheter or guidewire is positioned (pushed) at the entrance of the next branch at a vessel bifurcation. This process can take a few seconds to be completed.

3. Combining IGC-MRN with SGC-MRN

The IGC can be combined with the SGC to form what is referred to as a double-insert, as depicted in Fig. 2. In this

case, the IGC is inserted inside the SGC and the double-insert can be placed inside the tunnel of the clinical MRI scanner to take advantage of the B_0 field.

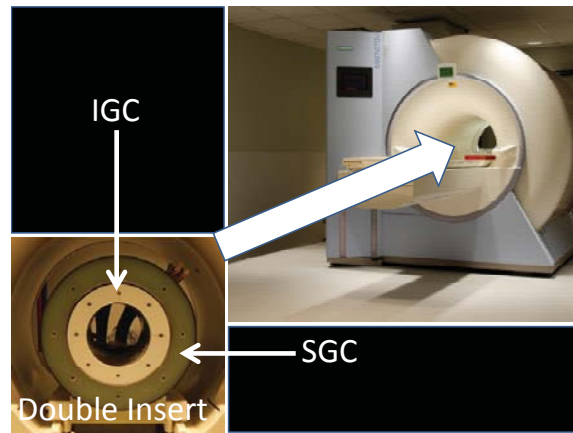


Figure 2. Photograph of the double-insert showing the IGC inside the SGC

With the double-insert, the advantages of both approaches are available for MRN. The choice to use IGC-MRN or SGC-MRN with such a double-insert will depend on the vascular characteristics along the planned trajectory as well as the characteristics of the navigable agents. A simple example to demonstrate the fundamental principle is shown in Fig. 3.

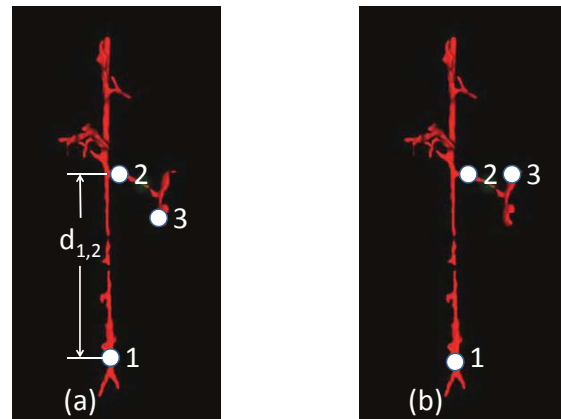


Figure 3. MR-images of the right and left renal and mesenteric arteries showing two possible scenarios ((a) and (b)) for MRN along waypoints 1, 2 and 3

In Fig. 3a, SGC-MRN is a potentially viable alternative where the navigable agents could take advantage of a longer duty cycle for steering purpose along the distance separating two successive waypoints (e.g., $d_{1,2}$ between waypoints 1 and 2 in Fig. 3a) and where the direction of the steering gradient can remain unchanged between waypoints 1 and 3.

In Fig. 3b, a change in the steering gradient is necessary between waypoints 2 and 3. In this particular case, considering the blood velocity and the shorter distance

separating waypoints 2 and 3, it becomes obvious that insufficient time is available to switch the direction of the SGC. In this case, IGC-MRN is likely to be more efficient than SGC-MRN provided that the first bifurcation towards waypoint 2 can be achieved with the IGC. Another alternative is to use the SGC to perform magnetically steered catheterization in the segment $d_{1,2}$ in order to bring the tip of the catheter at waypoint 2, where the navigable agents would be released prior to performing SGC-MRN, towards waypoint 3 in Fig. 3b. If deeper MRN must be performed towards another waypoint beyond waypoint 3 requiring a directional change of the steering gradient, then IGC-MRN could replace SGC-MRN after releasing the navigable agents at the tip of the catheter.

4. MR-Navigable Therapeutic Agents

MR-navigable therapeutic agents can take various forms. Initial proofs-of-concept were done using MRN agents known as TMMC, which, as mentioned earlier, consist of cancer therapeutics known as Doxorubicin (DOX) embedded with FeCo magnetic nanoparticles (MNP) within a spherical biodegradable polymer (PLGA) matrix. More specifically, FeCo nanoparticles, coated with a 10-nm graphite shell, exhibited a diameter (\varnothing) of 206 ± 62 nm and M_s of 195 ± 10 emu g^{-1} . TMMC were loaded (% w/w) with DOX (3.2 ± 0.5) and FeCo nanoparticles (37 ± 2.7) exhibited the following properties: $\varnothing = 53 \pm 19$ μm , $M_s = 72 \pm 3$ emu g^{-1} and a sustained drug release over several days.

Several versions of TMMC could be synthesized, each version having a different ratio of magnetic materials versus therapeutic loads. Indeed, increasing the amount of drug in each MRN-agent within the limit of the synthesis process would yield a higher density of therapeutics to be delivered for a given number of agents being injected. On the other hand, by doing so, the amount of MNP per agent would be decreased, which would reduce the effect of the gradient forces from the MRN system. But increasing the amount of MNP per agent would also increase the dipole-dipole interactions between neighbored agents, forming chain-like aggregates in the shape of prolate ellipsoids with the longitudinal axis oriented towards the z-axis of the MRN platform. When navigating TMMC parallel to the z-axis, applying too much gradient may increase the friction force between the TMMC aggregates and the vessel's wall; this would influence the steering efficacy at the next blood vessel's bifurcation. When navigating perpendicular to the z-axis, such aggregates could have lengths extending beyond the diameter of the next branching vessel. In this case, if the blood flow is too weak, premature embolization of the blood vessels could occur where the TMMC aggregates would not proceed further towards the targeted site. With sufficient blood

flow providing the force necessary to break the dipole-dipole interactive force between TMMC in the aggregates, a fraction of each aggregate could lead to the other branching vessel resulting in a lower targeting efficacy while increasing the systemic toxicity level for the patient. Therefore, although the high gradients and extended duty cycles are necessary to achieve adequate targeting efficacy, caution must be practised so that the characteristics of the navigable agents, the physiological conditions and in particular the blood flow rate, as well as the length of the vessel's segments and the direction of the navigable agents with regard to the z-axis, are all taken into account.

5. Discussion

The results obtained indicate that implementing a whole-body IGC or SGC capable of achieving sufficiently high gradients for steering navigable agents in the arterioles is not a trivial task, due to technological limits. In the shorter term, IGC-MRN and SGC-MRN could be conducted in the limbs or the head where the diameter of the IGC or SGC can be decreased, facilitating the implementation of coils capable of generating steering gradients with adequate slew rates and amplitudes. Unlike for SGC-MRN, IGC-MRN could affect the patient by generating gradients well above the threshold for peripheral nerve pain. This suggests that IGC-MRN sequences within FDA recommendations could be made from alternate imaging and steering sequences where MRI sequences have a maximum amplitude of 90 mT \cdot m $^{-1}$ and rise time of 200 μs , and steering gradients have a maximum amplitude of 450 mT \cdot m $^{-1}$ and rise time of 22.5 ms.

Catheterization has the potential to help MRN effectiveness by injecting the navigable agents deeper and at strategic locations. To do so, a magnetically guided catheterization procedure using the SGC or potentially the IGC would be a great addition to MRN-based intervention suggesting the use of a double-insert for many cases. Such a double-insert takes up more volume in the tunnel of a clinical MRI scanner and therefore restricts the maximum diameter of the IGC. Although reducing the diameter of the IGC helps in achieving imaging gradients with proper specifications, such reductions in diameter may limit the regions of the body that could be treated, unless a dedicated MRN platform is developed.

Our experience in MRN shows that the decision-making process can be difficult for medical staff; special software interfaces could therefore be helpful during the planning phase. Such software would take into account not only the characteristics of the navigable agents as well as the IGC and SGC, but also the physiological characteristics encountered between the planned injection and targeted sites.

Another aspect to consider is the number of repetitive injections to be performed. Indeed, depending on the therapeutic dose to be delivered, delivering the required dose in only one injection is unlikely. This is due to the constrained volume in narrower vessels and therefore the maximum quantity of navigable agents per injection. A number of injections may impact the heating of the coils or extend substantially the overall time required to conduct such MRN-based interventions.

Despite these constraints, MRN is a serious method for microrobotic-based targeted interventions in the vascular network compared to other proposed methods. For instance, piezoelectric ultrasonic micro-motors have been proposed and investigated for *in vivo* microrobotic applications [7]. The advantage of this approach is that no external source is necessary for generating the propulsive or steering force. On the other hand, scaling may prove difficult. Indeed, although the authors claim that the cross-sectional dimension of the microrobot could be reduced down to 250 μm without loss of performance compared to a previous prototype with a diameter of 400 μm , these dimensions would restrict applications in the arteries only. Another concern is the maximum therapeutic payloads that could be delivered from such a device, considering that only one device can operate in the artery at a given time. The fact that the device is not made of biodegradable materials suggests that its recovery would be required and since piezo-actuation also requires relatively high voltage, this would pose further challenges for implementing untethered versions. Nonetheless, such technology is promising for other applications in the arteries.

In [8], the authors propose a platform referred to as the EMA system which is based on a pair of stationary Helmholtz-Maxwell coils and a pair of rotational Helmholtz-Maxwell coils for manipulating a microrobot in a 3-dimensional space. A uniform magnetic flux density is provided by the Helmholtz coils with the gradients being provided by the Maxwell coils. The advantage of this platform is that the torque acting on the microrobot is not constrained to a single direction, as is the case for MRN. Although this can be an advantage for shape-anisotropic microrobots, it is not a significant advantage for spherical implementations such as the TMMC or other potential shape-isotropic microrobots. Although the platform would allow rotational control of needle-like aggregates of TMMC, MR-imaging during the interventions would have to be replaced by other medical imaging modalities without enhanced tissue contrast, which is important in such target interventions. The system is also bulky and makes it difficult to generate higher fields within an appropriate workspace for soft magnetic materials with a high magnetization saturation level. This may necessitate the use of permanent magnets in the microrobot or the use of a larger volume of soft

magnetic material; in both cases this would lead to larger microrobots that might be constrained to navigate in larger arteries. The rotational movement of the coils also reduces the response time to re-align the field, which may be a constraint on achieving the required real-time performance. Nonetheless, the EMA system has advantages that may prove to be suitable for specific types of interventions conducted in arteries.

In [9], a permanent magnet attached to a robotic arm is used to generate a magnetic gradient for locomotion and navigation based on magnetic dragging of MNP-based devices for the treatment of vascular obstructions. The main advantage of such a platform is its relative simplicity and relatively low cost. But since it relies on a magnetic gradient only, it may be difficult to achieve full magnetization of the MNP or to fully exploit MNP with high magnetization saturation levels unless operating relatively close to the external magnet. As such, the method could be most appropriate for operation in arteries where the volume of magnetic material can be increased to compensate for interventions being performed deeper in the body. The fact that the gradient is generated by the mechanical displacement of an external magnet may have a significant impact on the real-time performance of switching the direction of the gradient for target drug deliveries. But for particular interventions conducted in the arteries, such as the treatment of vascular obstruction, the method may prove to be adequate.

Another interesting platform is the OctoMag system [10]. The platform accomplishes a very high level of wireless control through a relatively large workspace characterized by complex non-uniformed magnetic fields by exploiting linear representations of coupled field distributions of multiple soft-magnetic-core electromagnets acting in concert. The system has the potential to be scaled up for human interventions with magnetic gradients comparable to the MRN platform but with a much lower magnetic field at the centre of the workspace. Indeed, instead of a 1.5 T or higher field, the field might be as low as 0.1 T. At such a level, with the magnetization curve of soft-magnetic MNP characterized by high magnetization saturation, this may translate to a relatively low induced force, which would be compensated by larger microrobots. But considering the difficulty in scaling the MRN platform for an inner diameter capable of accepting a human adult, such an approach may prove quite efficient for particular wireless interventions in the arteries or for magnetic-based catheterization procedures.

6. Conclusion

Medical micro-nanorobotics in the vascular network is a new field of research that has shown potential in target

interventions such as in cancer therapies and diagnostics. Although the use of magnetic fields already implemented in upgraded clinical MRI scanners is a promising approach for servoing navigation control of navigable agents in the vascular network, improvement in cooling of the coils for extending the duty cycles, as well as improvement in MR-tracking algorithms, would certainly help in translating this technology to whole-body MRN. Nonetheless, experimental results already show great potential for this technology for contributing to enhanced therapeutic efficacy while reducing severe secondary toxicity for the patients.

7. Acknowledgements

The author acknowledges the participation of the members of the NanoRobotics Laboratory, Dr Soulez and Dr Beaudoin from the Centre Hospitalier de l'Université de Montréal (CHUM) during the *in vivo* experiments. At the time of the writing, the author was supported by the Research Chair of École Polytechnique in Nanorobotics and a Discovery Grant from the National Research Council of Canada (NSERC). The equipment used in this study was acquired with a grant from the Canada Foundation for Innovation (CFI).

8. References

- [1] Jain KK (2005) Editorial: Targeted drug delivery for cancer. *Technology in Cancer Treatment*. 4(4), 311-313.
- [2] Mathieu JB, Beaudoin G, Martel S (2006) Method of propulsion of a ferromagnetic core in the cardiovascular system through magnetic gradients generated by an MRI system. *IEEE Trans. on Biomed. Eng.* 53(2), 292-299.
- [3] Martel S, Mathieu JB, Felfoul O, Chanu A, Aboussouan É, Tamaz S, Pouponneau P, Beaudoin G, Soulez G, Yahia L'H, Mankiewicz M (2007) Automatic navigation of an untethered device in the artery of a living animal using a conventional clinical magnetic resonance imaging system, *Appl. Phys. Lett.* 90, 114105.
- [4] Pouponneau P, Leroux JC, Soulez G, Gaboury L, Martel S (2011) Co-encapsulation of magnetic nanoparticles and doxorubicin into biodegradable microcarriers for deep tissue targeting by vascular MRI navigation. *Biomaterials*. 32(13), 3481-3486.
- [5] Schaefer DJ, Bourland JD, Nyenhuis JA (2000) Review of patient safety in time-varying gradient fields. *J. Magn. Reson. Imaging*. 12, 20-29.
- [6] Price RR (1999) The AAPM/RSNA physics tutorial for residents: MR imaging safety considerations. *RadioGraphics*. 19, 1641-1651.
- [7] Watson B, Friend J, Yeo L (2010) Modelling and testing of a piezoelectric ultrasonic micro-motor suitable for *in vivo* micro-robotic applications. *J. Micromech. Microeng.* 20, 115018-115033.
- [8] Jeong S, Choi H, Choi J, Yu C, Park J, Park S (2010) Novel electromagnetic actuation (EMA) method for 3-dimensional locomotion of intravascular microrobot. *Sensors and Actuators A: Physical*. 157(1), 118-125.
- [9] Tognarelli S, Castelli V, Ciuti G, Di Natali C, Sinibaldi E, Dario P, Menciassi A (2012) Magnetic propulsion and ultrasound tracking of endovascular device. *J. Robotic Surgery*. 6(1), 5-12.
- [10] Kummer MP, Abbott JJ, Kratochvil BE, Borer R, Sengul A, Nelson BJ (2010) OctoMag: An electromagnetic system for 5-DOF wireless micromanipulation. *IEEE Trans. Robotics*. 26(6), 1006-1017.